Quantum Interference in LaB_6

N. Harrison,[1] R. G. Goodrich,[2] J. J. Vuillemin,[3] Z. Fisk,[4] and D. G. Rickel[1]
[1]*National High Magnetic Field Laboratory, LANL, MS-E536, Los Alamos, New Mexico 87545*
[2]*Department of Physics and Astronomy, Louisiana State University, Baton Rouge, Louisiana 70803*
[3]*Department of Physics, University of Arizona, Tucson, Arizona 85721*
[4]*National High Magnetic Field Laboratory, Florida State University, Tallahassee, Florida 32310*
(Received 08 December 1997)

Quantum interference effects in the induced currents in metallic LaB_6 are investigated in pulsed magnetic fields extending to 60 T and to temperatures of up to 70 K. One of the quantum interference frequencies, corresponding to an area in k space equal to the Brillouin zone, has an effective mass precisely equal to *zero*. The attenuation of this and other frequencies at high temperatures requires the scattering effects of phonons to be considered within the Boltzmann transport equation. [S0031-9007(98)06150-X]

PACS numbers: 71.18.+y, 72.10.Fk, 72.15.Gd

The quantum interference (QI) of electrons within magnetic breakdown (MB) networks is a rare phenomenon in metals [1–3]. The Stark interferometer concept was originally devised to explain transport phenomena in pure Mg [1–3]. The effect has since been found to readily manifest itself in low-dimensional (LD) organic charge-transfer salts [4–6], but there have been no further reports in conventional three-dimensional (3D) metals. When interference occurs, the k-space area A_j enclosed by the interferometer appears as a "virtual" Onsager phase within the Boltzmann transport equation, leading to new frequencies in addition to the conventional Shubnikov–de Haas (SdH) oscillations [2–4,7]. It is generally understood that QI does not manifest itself in thermodynamic properties of the system [2–4,7] and so cannot contribute to magnetic oscillations giving rise to the de Haas–van Alphen (dHvA) effect. In spite of this, QI oscillations in the magnetotransport behave in a manner that is in remarkable concordance with the Lifshitz-Kosevich (LK) theory [8] of Landau quantum (LQ) oscillations. As with LQ oscillations, the effective mass m_j^* associated with the enclosed area A_j is proportional to the energy derivative $\partial A_j/\partial \epsilon_k$ [2–4], where ϵ_k is electron energy. An unusual situation arises when A_j has a weak or negligible dependence on ϵ_k so that m_j^* is anomalously small, as has been shown to occur both in pure Mg [1–3] and in the organic superconductor κ-$(BEDT\text{-}TTF)_2Cu(NCS)_2$ under hydrostatic pressure [9]. Because the net effective mass is small, QI oscillations persist to high temperatures where the conventional SdH oscillations with much higher effective masses are completely damped.

In this Letter we report a particularly novel situation in LaB_6 where not only are QI oscillations observed in a 3D metal, but where one of the QI frequencies corresponds exactly to the cross-sectional area of the Brillouin zone (BZ) with an effective mass precisely equal to zero. The Fermi surface (FS) of LaB_6 primarily consists of prolate electron ellipsoids centered at the X points of the cubic BZ, connected together by short necks [10,11]. The extremal cross-section area of these ellipsoids within the XMR plane of the BZ (referred to as the α_3 branch in Ref. [11]) accounts for the majority of the dHvA signal at low magnetic fields. Weaker signals originate from closed hole orbits within the ΓXM plane (which we will refer to as ε and γ following common usage); all of these orbits are illustrated in Fig. 1. A second sheet of the FS consists of a set of eight smaller electron ellipsoids located within the necks [12]. At sufficiently strong magnetic fields, MB through the necks, involving the smaller ellipsoids, leads to a multitude of new frequencies. The simplest MB orbit $\alpha_{1,2} + 2\rho$ within the ΓXM plane is illustrated

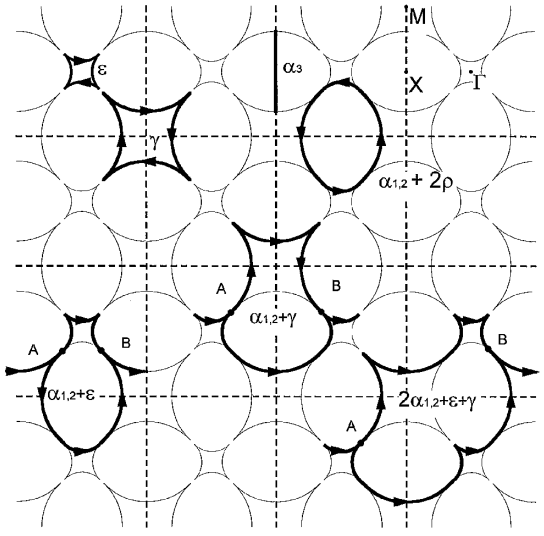

FIG. 1. A cross section of the Fermi surface of LaB_6 through the ΓXM plane in the extended zone representation. The hole orbits ε and γ are shown together with the simplest MB orbit $\alpha_{1,2} + 2\rho$. The intersection of the α_3 extremal orbit, which occurs within the XMR plane, is indicated by a heavy line. In addition, we schematically illustrate possible orbits for the three principal QI areas. The heavy circles indicate the points at which the QI paths divide (A) and recombine (B).

 0031-9007/98/80(20)/4498(4)$15.00

in Fig. 1; each small ellipsoid contributes only ~2.5 T, and is therefore too small to be seen in Fig. 1. The three principal areas enclosed between two interfering electrons on trajectories within this plane are also illustrated in Fig. 1. Of these, the $\alpha_{1,2} + \varepsilon$ and $\alpha_{1,2} + \gamma$ combination frequencies are expected to have finite effective masses as listed in Table I; note that the contributions from the smaller electron ellipsoids cancel for the two branches. Since the BZ contains exactly two $\alpha_{1,2}$ areas, an ε orbit and a γ orbit, it is evident from the QI paths shown in Fig. 1 that the $2\alpha_{1,2} + \gamma + \varepsilon$ combination frequency corresponds to the area A_{BZ} of the BZ. The absence of an associated effective mass for this QI area originates from the fact that this area is independent of ϵ_k. This situation, where $m_j^* \equiv 0$, is presently unique to LaB_6.

While QI should be a universal feature of all MB networks, the lack of observation of QI in 3D high conductivity metals primarily concerns the difficulty in measuring the SdH effect in such systems. The SdH effect represents only a tiny fraction of the total magnetoresistance, which is itself very small. LaB_6 certainly falls within the category of high conductivity metals [13], possessing large FS sheets and low quasiparticle effective masses [10]. In such metals where conventional resistance measurements may lack the required sensitivity, the inductive technique in pulsed magnetic fields provides an alternative [14]. In a pulsed field experiment, induced eddy currents in the sample contribute to its measured magnetic moment m in addition to the dHvA effect. The total induced voltage in the detection coils is $v = \eta(\partial m/\partial t) \equiv \eta(\partial B/\partial t)(\partial m/\partial B)$, where η is the geometrical coupling factor of the sample to the detection coils. For a cylindrical sample of radius a and length l, the eddy current magnetic moment is given by $m_{\mathrm{ed}} = \int_0^a J(x)\pi l x^2 dx$ where $J(x) = E(x)/\rho$ is the radial current density and $E(x) = (x/2)\,dB/dt$. If the resistance is assumed to take the form $\rho \approx \bar{\rho}(1 + \sum_i c_j \cos[2\pi F_j/B + \phi_j])$ [4], where c_j is the ratio of the oscillatory resistance to the background resistance $\bar{\rho}$, it follows that each SdH or QI frequency F_j contributes an eddy-current susceptibility

$$\frac{\partial m_{\mathrm{ed},j}}{\partial B} \approx \frac{\pi l a^4}{8\bar{\rho}}\left(\frac{\partial B}{\partial t}\right) c_j \frac{2\pi F_j}{B^2} \sin\left[\frac{2\pi F_j}{B} + \phi_j\right]. \quad (1)$$

The LaB_6 used for this study was grown using the method described in Ref. [10]. Pulsed magnetic fields to 60 T were provided by the National High Magnetic Field Laboratory, Los Alamos, while temperatures between 1.5 and 80 K were obtained by carefully controlling the heat input into a closed volume of ^{4}He gas, vacuum separated from a main bath of ^{4}He liquid. The temperature was measured by means of a Lakeshore Cernox resistor mounted close to the sample.

A Fourier transformation (FT) of the oscillatory magnetization on the falling field at 1.5 K is shown in Fig. 2(a). At low temperatures, where the dHvA effect dominates, the rich spectrum of frequencies originates not only from direct extremal orbits and their harmonics, but also from MB and the Shoenberg magnetic interaction (MI) effect [15]. Frequencies originating solely from MI can be identified as those corresponding to combinations of frequencies from planes intersecting the cubic BZ at different values of k_z; k_z being the k vector parallel to B. It should be noted that the frequencies identified with QI in Fig. 1 can also be generated by MI. Only at higher temperatures, where the dHvA oscillations become significantly damped, is MI no longer a factor. The FT of the oscillations at 50 K in Fig. 2(b) clearly indicates that the amplitudes of the dHvA contributions are considerably attenuated. The three principal frequencies that remain correspond to the QI trajectories illustrated in Fig. 1. We can discriminate between oscillations in the induced eddy currents and dHvA oscillations by observing their phase on the rising and falling magnetic fields. The dHvA magnetization is a static effect (independent of $\partial B/\partial t$), but since $v \propto \partial B/\partial t$, the phase of the dHvA signal reverses between rising and falling fields. This is apparent in the inset of Fig. 2(a) in which the dHvA effect dominates. On the other hand, the voltage induced from oscillations in the magnetoresistance is proportional to $(\partial B/\partial t)^2$. In this case, the induced voltage oscillations maintain the same phase irrespective of the direction of sweep of the magnetic field, as is apparent from the oscillations measured at 50 K in the inset of Fig. 2(b).

In spite of the fact that the BZ frequency is predicted to have an effective mass of zero, it is evident from Fig. 3 that all of the QI frequencies have notable temperature dependences. The amplitudes of all three frequencies change by more than 2 orders of magnitude between 20 and 70 K. Clearly this cannot be accounted for by renormalizing by the temperature dependence of $\bar{\rho}$ alone. Even in the absence of a magnetic field, the resistivity changes by little more than 1 order of magnitude between

TABLE I. A list of thermal effective masses m^* and also the mass m', which enters into the transport scattering term, for the three principal QI frequencies.

QI frequency	m^*	m'
$\alpha_{1,2} + \varepsilon$	$m_\varepsilon^* - m_{\alpha 1,2}^* = 0.18$	$m_\varepsilon^* + \frac{1}{2}m_{\alpha 1,2}^* = 1.21$
$\alpha_{1,2} + \gamma$	$m_{\alpha 1,2}^* - m_\gamma^* = 0.18$	$\frac{1}{2}m_\varepsilon^* + m_{\alpha 1,2}^* = 1.03$
$2\alpha_{1,2} + \varepsilon + \gamma = \mathrm{BZ}$	$2m_{\alpha 1,2}^* - m_\varepsilon^* - m_\gamma^* = 0$	$\frac{5}{4}m_\varepsilon^* + \frac{5}{4}m_{\alpha 1,2}^* = 1.87$

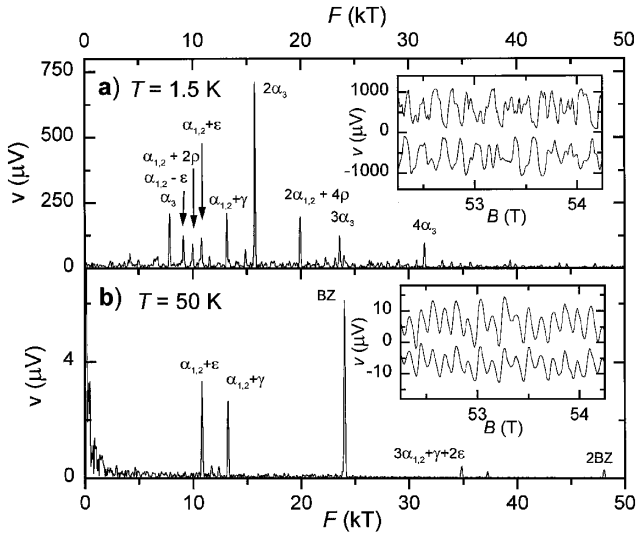

FIG. 2. (a) A Fourier transformation of the dHvA signal measured in LaB_6 at 1.5 K on the falling magnetic field for the interval in the field between 30 and 60 T. The inset shows part of the induced voltage signal which appears noisy owing to the multitude of MB frequencies together with QI oscillations. The dHvA component, which dominates at low temperatures, reverses phase between rising and falling fields (offset for clarity). (b) A Fourier transform of the signal measured in LaB_6 at 50 K over the same interval as (a). Part of the actual QI oscillations are shown in the inset. Note that the QI oscillations maintain the same phase irrespective of the sign of $\partial B/\partial t$.

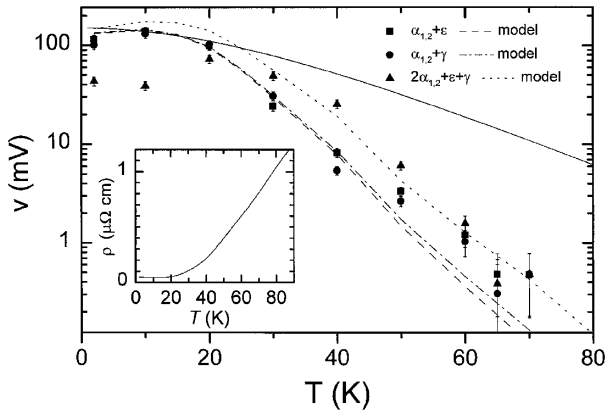

FIG. 3. The temperature dependences of the QI frequencies in LaB_6. The solid line represents the expected temperature dependence for the $\alpha_{1,2} + \varepsilon$ and $\alpha_{1,2} + \gamma$ frequencies, not including any possible temperature dependence of τ_t. The dashed and dotted lines show the expected temperature dependences on incorporating the temperature dependence of τ_t as inferred from the resistivity [13] shown in the inset. The errors are estimated from the background noise of the FT.

2 and 70 K [13]. The main features of the magnetoresistance can be understood by considering the expression

$$\overleftrightarrow{\sigma} = e^2 \int \frac{d^3k}{4\pi^3}\left(-\frac{\partial f}{\partial \varepsilon}\right) v_k \Lambda_k \qquad (2)$$

for the transverse conductivity, as derived from the linearized Boltzmann transport equation [3]. The essential features of the SdH effect depend on the velocity v_k, which is a function of the density of states. Since the broadening of the energy levels is determined by the quantum lifetime τ_q, the SdH oscillations conform to the LK formalism in much the same way as the dHvA effect [8]. QI effects, on the other hand, are a manifestation of the mean free displacement $\Lambda_k = \int_{\infty}^{t_0(t)} v_k(t) \exp[(t - t_0)/\tau_t] dt$ [3], which is a summation over all possible paths throughout the MB network. Since Eq. (2) describes the semiclassical magnetotransport, Λ_k is determined by the transport scattering time τ_t. In Ref. [4] it was shown that QI introduces oscillatory contributions

$$\tilde{P}_j = 2p^{n1}q^{n2} \cos\phi_j \exp(-\pi/\omega_j'\tau_t) \qquad (3)$$

to the flux of carriers between two points. Adopting the notation developed by Falicov and Stachowiak [16], $P = p^2$ and $Q = q^2$ are the MB and Bragg reflection probabilities, respectively, and $n1$ and $n2$ are the respective number of nodes at which MB and Bragg reflection occur.

It follows from Eq. (3) that there are two contributions to the temperature dependence of the oscillations. Since the phase $\phi_j = \hbar A_j/eB$ can be a function of ϵ_k as well as B, upon integration over ϵ_k, the Fermi-Dirac distribution f smears the ϵ_k-dependent phase contributions of Λ_k, to result in the conventional thermal damping factor $X_j/\sinh X_j$ [15], where $X_j = 2\pi^2 r k_B m_j^* T/\hbar eB$ (r being the harmonic index). The mass enhancement due to the electron-phonon (e-ph) interaction should therefore be the same for the QI oscillations as it is for the LQ oscillations. In the quantum mechanical picture, it is well established that the (e-ph) interaction does not contribute to τ_q. Instead, the density of electronic states at the Fermi energy increases, resulting in an increase of the effective mass m_j^* relative to the band mass m_b by a factor $(\lambda + 1)$, where λ parametrizes the strength of the (e-ph) interaction [17]. Comparisons of the measured effective masses in LaB_6 with those from the calculated band structure indeed suggest a strong (e-ph) coupling [10], with $\lambda \sim 0.53$. Considering only the above effect of the Fermi-Dirac distribution on the QI oscillations, the solid line in Fig. 3 illustrates the temperature dependence that should be expected for the $\alpha_{1,2} + \varepsilon$ and $\alpha_{1,2} + \gamma$ QI frequencies for the effective masses given in Table I [18]. Evidently, the thermal smearing effects of the Fermi-Dirac distribution are not sufficient to account for the observed temperature dependence of any of the QI frequencies, let alone that of the zero mass BZ frequency.

The second contribution to the temperature dependence originates directly from τ_t. Unlike τ_q, τ_t includes the effects of phonon scattering. This difference originates from the fact that τ_q represents only the quantum lifetime of electrons on closed orbits within the Landau levels and does not translate directly to the actual motion of carriers throughout the metal. Previous investigations of QI effects have been made at temperatures far below the Debye temperature, where the number of phonons is still very low [1,3,4,6,9]. While LaB_6 is a relatively hard

material, the resistivity in the inset of Fig. 3 indicates a notable phonon contribution to the scattering at temperatures above ~20 K [13], becoming particularly strong by 70 K. To a first approximation, the phonon-modified transport scattering rate can be estimated by applying the Drude formula $\rho_{B=0} = m^*/e^2 n\tau_t$ to the measured resistivity (Fig. 3 inset) in the absence of a magnetic field. For this we can assume a FS-averaged mass of $m^* \sim 0.65 m_e$, while the carrier density n corresponds to exactly one electron per unit cell. The period $1/\omega_j' = m_j'/eB$ is the sum of the times taken for the carriers to complete each branch of the QI orbit. This defines a scattering effective mass m_j' which is equal to the sum of the masses of the two branches and is therefore different from the thermal effective mass m_j^*. Upon incorporating the additional temperature dependence of τ_t into the amplitude reduction shown in Fig. 3, the theoretical temperature dependences (shown by dotted and dashed lines) now reproduce the experimental temperature variation more closely. In this model, the temperature dependence of the induced voltage now has the form $v_j \propto R_T \exp[-\pi/\omega_j'\tau_t]/\bar{\rho}$. Since LaB_6 has only a very small magnetoresistance when the field is oriented along the $\langle 100 \rangle$ axis [20], we have used the zero field values of $1/\bar{\rho}$. It should be noted that the values of τ_t estimated from ρ in this work were inserted directly into the above expression for v_j without any adjustment. In contrast, an interpretation of the "rapid oscillation" effect in LD $(TMTSF)_2ClO_4$ by Uji *et al.* [6] in terms of QI had yielded notable discrepancies between the values of τ_t obtained from the temperature dependences of the QI and ρ [19]. While there are some inconsistencies with the application of the QI model to $(TMTSF)_2ClO_4$ (for example, this does not explain why oscillations of the same frequency appear in the magnetization [6]), LaB_6, on the other hand, has a simple 3D metallic ground state for which the FS is well understood [11–13]. One feature of our experimental results that cannot be explained by the model is the apparent loss of amplitude (of up to 40%) of the BZ frequency below 30 K. One obvious possibility is that the BZ frequency differs by only (1–2)% from the third harmonic of the α_3 frequency, which is the more dominant at low temperatures and can lead to spurious amplitudes in the FT.

In summary, investigations of the magnetization of LaB_6 in pulsed magnetic fields of up to 60 T reveal the presence of QI effects within the induced eddy currents. The temperature dependence of one of the frequencies, which corresponds to an area equal to that of the BZ and has a thermal effective mass of zero, requires the temperature dependence of τ_t to be considered within the Boltzmann transport equation. Finally, we note that oscillations at the BZ frequency have been observed in pure Sn [21], and were attributed to Pippard's "zone oscillation" effect [22]. The Fermi surface of Sn does, however, allow the possibility of QI, including an enclosed area equal to that of the BZ, as is the case in LaB_6. Given that the BZ frequency in Sn has been reported only in the magnetoresistance and is also observed to have an "anomalously low effective mass," QI appears to be the more likely explanation.

Work conducted at the National High Magnetic Field Laboratory was supported by the National Science Foundation (NSF), the State of Florida, and the Department of Energy. Additional support from the NSF (No. DMR95-01419) is acknowledged by one of us (R. G. G). One of the authors (J. J. V.) thanks Professor R. W. Stark for useful discussions.

[1] R. W. Stark and C. B. Friedberg, Phys. Rev. Lett. **26**, 556 (1971); J. Low Temp. Phys. **14**, 111 (1974).
[2] R. W. Stark and R. Reifenberger, J. Low Temp. Phys. **26**, 763 (1977).
[3] D. Morrison and R. W. Stark, J. Low Temp. Phys. **45**, 531 (1981).
[4] N. Harrison *et al.*, J. Phys. Condens. Matter **8**, 5415 (1996).
[5] A. A. House *et al.*, J. Phys. Condens. Matter **8**, 10 361 (1996); A. A. House *et al.*, J. Phys. Condens. Matter **8**, 10 377 (1996).
[6] S. Uji *et al.*, Phys. Rev. B **53**, 14 399 (1996).
[7] M. I. Kaganov and A. A. Slutskin, Phys. Rep. **98**, 189 (1983).
[8] I. M. Lifshitz and A. M. Kosevich, Sov. Phys. JETP **2**, 636 (1956).
[9] M. V. Kartsovnik *et al.*, Phys. Rev. Lett. **77**, 2530 (1996).
[10] A. J. Arko *et al.*, Phys. Rev. B **13**, 5240 (1976).
[11] Y. Ishizawa *et al.*, J. Phys. Soc. Jpn. **42**, 112 (1977).
[12] Y. Ishizawa *et al.*, J. Phys. Soc. Jpn. **48**, 1439 (1980).
[13] I. Bat'ko *et al.*, J. Alloys Compd. **217**, L1 (1995).
[14] This technique has recently been applied to investigate eddy-currents "resonances" in α-$(BEDT\text{-}TTF)_2TlHg(SCN)_4$ [N. Harrison *et al.*, Phys. Rev. Lett. **77**, 1576 (1996)]. In that case, due to its high resistivity, we would not expect to see large oscillatory eddy currents. They appear due only to the near vanishing of the in-plane magnetoresistance due to the possible occurrence of the quantum Hall effect. Subsequent experiments in static fields have lent support to this explanation [N. Harrison *et al.*, Phys. Rev. B **55**, R16 005 (1997)].
[15] D. Shoenberg, *Magnetic Oscillations in Metals* (Cambridge University Press, Cambridge, England, 1984).
[16] L. M. Falicov and H. Stachowiak, Phys. Rev. **147**, 505 (1966).
[17] S. Engelsberg and G. Simpson, Phys. Rev. B **2**, 1657 (1970).
[18] The values of m^* for the ε and γ orbits derived from the band structure apply, although renormalized by $(\lambda + 1)$. The effective mass of the $\alpha_{1,2}$ component can be inferred from the relation $2m_{\alpha 1,2}^* = m_\varepsilon^* + m_\gamma^*$.
[19] It appears that m_j^* and m_j' were incorrectly assigned [6]. m_j^* was assumed to be zero without prior justification, while m_j' was assumed to have the mass of only one branch of the QI trajectory.
[20] Y. Ishizawa *et al.*, J. Phys. Soc. Jpn. **49**, 557 (1980).
[21] J. K. Hulbert and R. C. Young, Phys. Rev. Lett. **27**, 1048 (1971).
[22] A. B. Pippard, Philos. Trans. R. Soc. London A **256**, 217 (1964).